Quantum chaos manifestation in the axial channeling

N F Shul'ga[1], V V Syshchenko[2], V S Neryabova[2] and A Yu Isupov[3]

[1] Akhiezer Institute for Theoretical Physics of the NSC "KIPT", Akademicheskaya Street, 1, Kharkov 61108, Ukraine

[2] Belgorod State University, Pobedy Street, 85, Belgorod 308015, Russian Federation

[3] Laboratory of High Energy Physics (LHEP), Joint Institute for Nuclear Research (JINR), Dubna 141980, Russian Federation

E-mail: shulga@kipt.kharkov.ua, syshch@bsu.edu.ru, syshch@yandex.ru

Abstract. Energy levels of classically chaotic system demonstrate mutual repulsion described by Wigner distribution of distances between neighboring levels. The statistical properties of energy levels for the axially channeling electron in the system of [110] atomic strings of a silicon crystal are studied in the present report. The inter-level spacing distributions obtained by numerical calculation demonstrate satisfactory agreement with a theoretical predictions for chaotic systems.

1. Introduction

Quantum chaos means the study of semiclassical behavior of systems whose classical motion exhibits chaos [1]. The most prominent characteristic of that behavior is the statistics of energy levels. It was demonstrated in many cases [2] that the spacing s between adjacent (neighboring) levels satisfies Wigner distribution

$$p(s) = (\pi s/2D^2)\exp(-\pi s^2/4D^2) \tag{1}$$

(where D is the mean level spacing) for chaotic systems, while exponential (sometimes called as Poisson) distribution

$$p(s) = (1/D)\exp(-s/D) \tag{2}$$

for regular ones. The last case manifests itself as a tendency to group the levels into shells.

The hypothesis of universality of the distribution (1) for classically chaotic systems is tested in the present article for the case of axial channeling of fast electrons in crystals.

2. Transverse energy levels of axially channeling particles

When an electron is incident to the atomic string of the crystal under small angle ψ, it can be captured by the attractive potential of the string. The finite motion in such potential is called the axial channeling (see, e.g., [3, 4, 5]). This motion could be (with good accuracy) described as a motion in the uniform string potential $U(x, y)$ (i.e. the potential of the atomic string averaged along its axis z). The longitudinal (i.e. parallel to the string axis) component of the particle momentum $p_{\|}$ is conserved in such field. The motion in the transverse plane will be described in this case by the two-dimensional Schrödinger equation [3]

$$\hat{H}\Psi(x, y, t) = i\hbar\frac{\partial}{\partial t}\Psi(x, y, t) \tag{3}$$

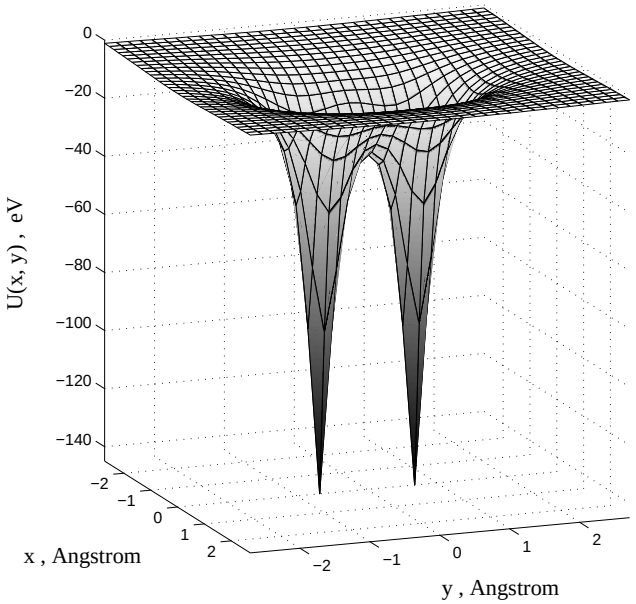

Figure 1. Electron potential energy (6) in the field of two neighboring atomic strings [110] of a silicon crystal.

with the Hamiltonian

$$\hat{H} = -\frac{\hbar^2}{2E_\parallel/c^2}\left(\frac{\partial^2}{\partial x^2} + \frac{\partial^2}{\partial y^2}\right) + U(x,y)\ , \tag{4}$$

in which the value $E_\parallel/c^2$ (where $E_\parallel = \sqrt{m^2c^4 + p_\parallel^2 c^2}$) plays the role of the particle mass.

The finite motion in the (x, y) plane would be characterized by the discrete set of the Hamiltonian (4) eigenvalues $E_\perp$. Such quantization of the transverse motion energy had been observed in many experiments for moderately fast electrons ($E_\parallel \sim 1$ MeV), when the total number of transverse energy levels is small (see, e.g., [4] and references therein).

The uniform string potential could be approximated by the formula [3]

$$U_1(x,y) = -U_0 \ln\left(1 + \frac{\beta R^2}{x^2 + y^2 + \alpha R^2}\right), \tag{5}$$

where for the [110] string of silicon $U_0 = 60$ eV, $\alpha = 0.37$, $\beta = 3.5$, $R = 0.194$ Å (Thomas-Fermi radius); the least distance between two parallel strings $a/4 = 5.431/4$ Å (where a is the lattice period). So, the uniform potential, in which the electron transverse motion takes place, will be described by two-well function (Figure 1)

$$U(x,y) = U_1(x, y + a/8) + U_1(x, y - a/8) \tag{6}$$

(neglecting the influence of far-away strings). The electron finite motion in such potential (corresponding to negative values of the transverse motion energy $E_\perp$) is known as axial channeling [3].

The potential (6) is suitable for quantum chaos investigations because the motion in such potential is classically chaotic if the transverse energy exceeds the saddle point of the potential well [5]. However, Schrödinger equation with such complicated potential as Eq. (6) requires numerical methods for its solution. In the present article we have found the transverse energy levels for axially channeling electrons in two-string potential (6) using the so-called spectral method [6], first applied to the channeling in [7, 8].

In brief, the method is based on the numerical simulation of the time evolution of initial wave function according to Schrödinger equation (3). The correlation function between wave functions at the initial and current time momenta, $\Psi(x, y, 0)$ and $\Psi(x, y, t)$,

$$P(t) = \int_{-\infty}^{\infty} \int_{-\infty}^{\infty} \Psi^*(x, y, 0)\Psi(x, y, t)\, dxdy, \tag{7}$$

contains information about the energy eigenvalues. Indeed, every solution of the time-dependent Schrödinger equation (3) could be expressed as the superposition

$$\Psi(x, y, t) = \sum_{n,j} A_{n,j} u_{n,j}(x, y) \exp(-iE_n t/\hbar) \tag{8}$$

of the Hamiltonian eigenfunctions $u_{n,j}(x, y)$,

$$\hat{H} u_{n,j}(x, y) = E_n u_{n,j}(x, y),$$

where the index j is used to distinguish the degenerate states corresponding to the energy E_n. Computation of the correlation function (7) for the wave function of the form (8) gives

$$P(t) = \sum_{n,n',j,j'} \exp(-iE_{n'}t/\hbar) A^*_{n,j} A_{n',j'} \int_{-\infty}^{\infty} \int_{-\infty}^{\infty} u^*_{n,j}(x, y) u_{n',j'}(x, y) dxdy =$$

$$= \sum_{n,n',j,j'} \exp(-iE_{n'}t/\hbar) A^*_{n,j} A_{n',j'} \delta_{nn'} \delta_{jj'} = \sum_{n,j} |A_{n,j}|^2 \exp(-iE_n t/\hbar). \tag{9}$$

Fourier transformation of (9) leads to the expression

$$P_E = \int_{-\infty}^{\infty} P(t) \exp(iEt/\hbar)\, dt = 2\pi\hbar \sum_{n,j} |A_{n,j}|^2\, \delta(E - E_n). \tag{10}$$

We see that the Fourier transformation of the correlation function looks like a series of δ-form peaks, positions of which indicate the energy eigenvalues.

However, integration of the numerically obtained correlation function $P(t)$ with the exponent in (10) could be carried out only over the finite time interval:

$$P_E = \int_0^T P(t) \exp(iEt/\hbar)\, dt = T \sum_{n,j} |A_{n,j}|^2 \exp(i(E - E_n)T/2\hbar) \operatorname{sinc}((E - E_n)T/2\hbar), \tag{11}$$

where $\operatorname{sinc}(x) = \sin(x)/x$. As a result, we obtain a series of peaks of finite width (inverse proportional to T) with sidelobes instead of infinitely narrow δ-like peaks (10). Employing normalized Hanning window function

$$w(t) = (1/T)(1 - \cos(2\pi t/T)) \tag{12}$$

in the integrand (11),

$$P_E = \int_0^T w(t) P(t) \exp(iEt/\hbar)\, dt, \tag{13}$$

substantially suppresses these sidelobes [6]. Typical correlation function shape in this case is presented in Figure 2.

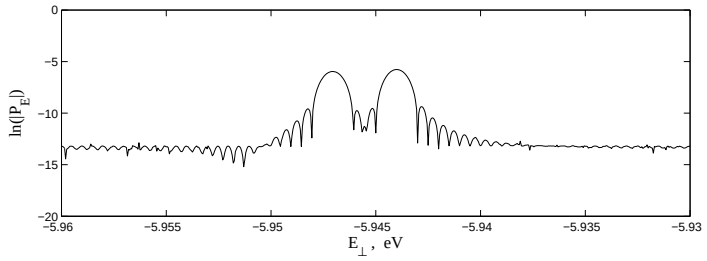

Figure 2. Correlation function (13) for electron of energy $E_{\|} = 400$ MeV with initial wave function (15) in the potential well (6) indicates two eigenvalues in the presented interval of transverse motion energy $E_{\perp}$.

Let two neighboring eigenvalues of $E_{\perp}$ are well-resolved in our numerical computation if not less than four side maxima are situated between two main ones. This leads to the criterion

$$T = 16\pi\hbar/\Delta E_{\perp} \tag{14}$$

for the total evolution time T necessary for the desirable energy levels resolution $\Delta E_{\perp}$. The resolution achieved in our computations is not worse than $\Delta E_{\perp} = 0.004$ eV. Further computational details are described in our previous papers [9, 10].

Note that the statistics of energy levels have to be studied separately for every type of eigenstate symmetry of the quantum system [2]. The potential well (6) has two planes of mirror symmetry: $x = 0$ and $y = 0$. So, every eigenstate of the electron in the potential (6) belongs to one of four classes of symmetry:

$$\Psi_{++}(-x, y) = \Psi_{++}(x, y), \quad \Psi_{++}(x, -y) = \Psi_{++}(x, y), \tag{15}$$

$$\Psi_{+-}(-x, y) = \Psi_{+-}(x, y), \quad \Psi_{+-}(x, -y) = -\Psi_{+-}(x, y), \tag{16}$$

$$\Psi_{-+}(-x, y) = -\Psi_{-+}(x, y), \quad \Psi_{-+}(x, -y) = \Psi_{-+}(x, y), \tag{17}$$

$$\Psi_{--}(-x, y) = -\Psi_{--}(x, y), \quad \Psi_{--}(x, -y) = -\Psi_{--}(x, y). \tag{18}$$

The level spacing distributions obtained for the semiclassical domain (close to the top of the potential well) demonstrate quite good agreement with the prediction (1) for every of these four symmetry classes. The distributions computed for the transverse energy domain

$$-10 \text{ eV} \le E_{\perp} \le -2.6 \text{ eV} \tag{19}$$

are presented in Figure 3. Small discrepancy could be caused by the limited statistics (the arrays of ~ 250 energy levels have been analyzed whereas the typical ones in [2] contain some thousands of levels).

Another possible reason of the mentioned discrepancy is a specific shape of the potential (6): rapid narrowing of the potential well with the depth increase leads to as much rapid increase of the average inter-level distance. Indeed, in the lower half of the energy interval (19)

$$-10 \text{ eV} \le E_{\perp} \le -6.3 \text{ eV} \tag{20}$$

the average inter-level distance D is about twice larger than in the upper one

$$-6.3 \text{ eV} \le E_{\perp} \le -2.6 \text{ eV}. \tag{21}$$

As a result, we can see better agreement of the distributions calculated for the intervals (21) and (20) with Wigner function (1) (Figures 4 and 5) than for the total interval (19).

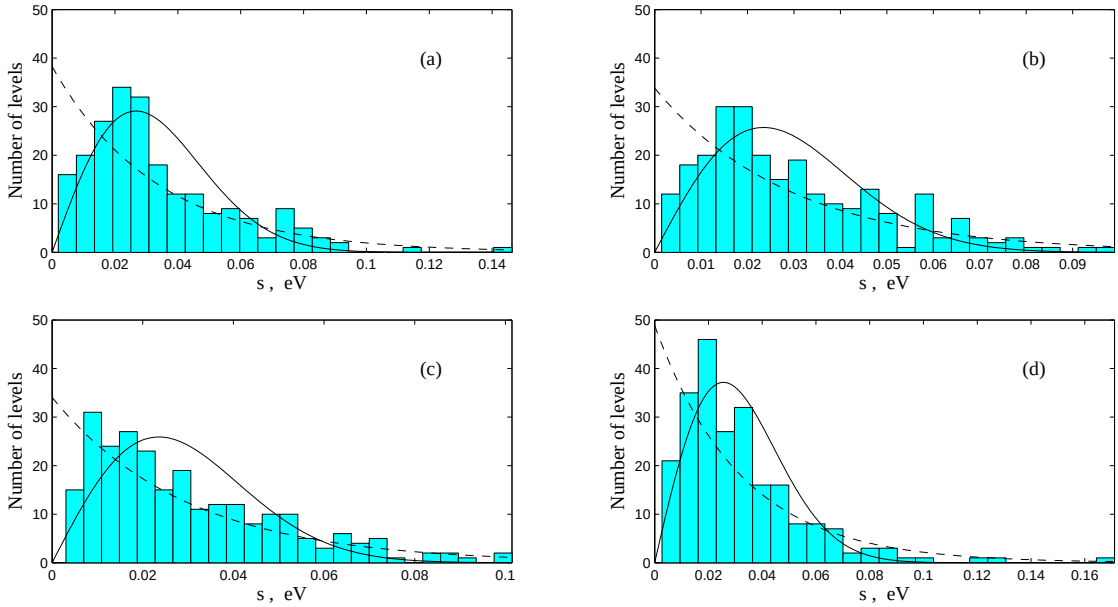

Figure 3. Transverse energy levels spacing distribution in the range (19) for $E_{\|} = 400$ MeV electrons channeled in the field of two parallel [110] strings of silicon crystal (histograms) as well as theoretical predictions (1) for chaotic motion (solid line) and (2) for regular motion (dashed line). The histograms are plotted for odd eigenstates (16), (17) (panels (a) and (b), respectively) and for even eigenstates (15), (18) (panels (c) and (d), respectively).

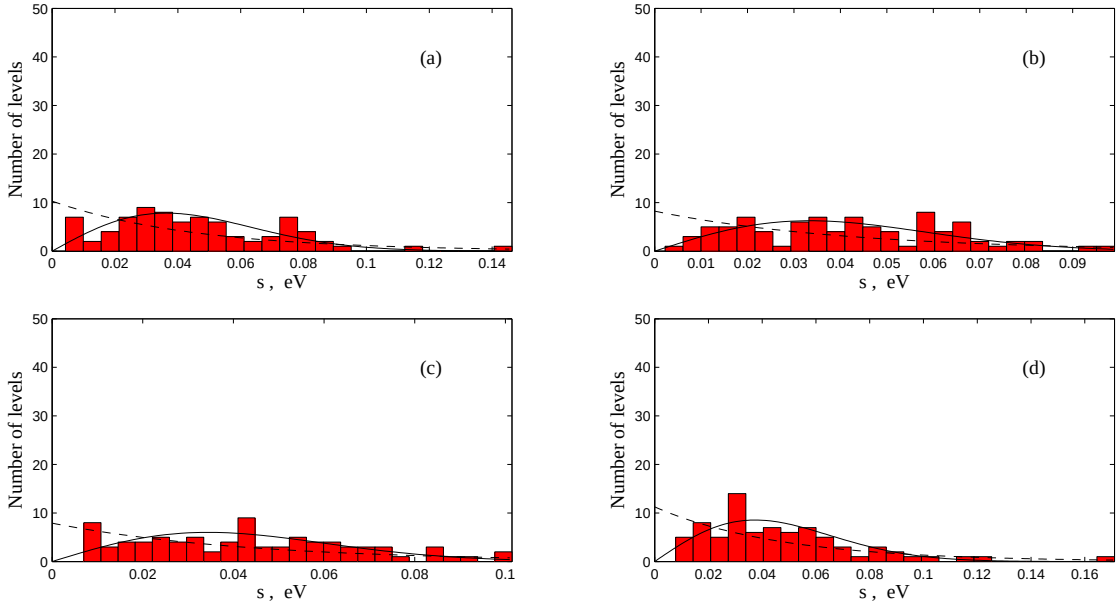

Figure 4. The same as in Figure 3 for the transverse energy domain (20).

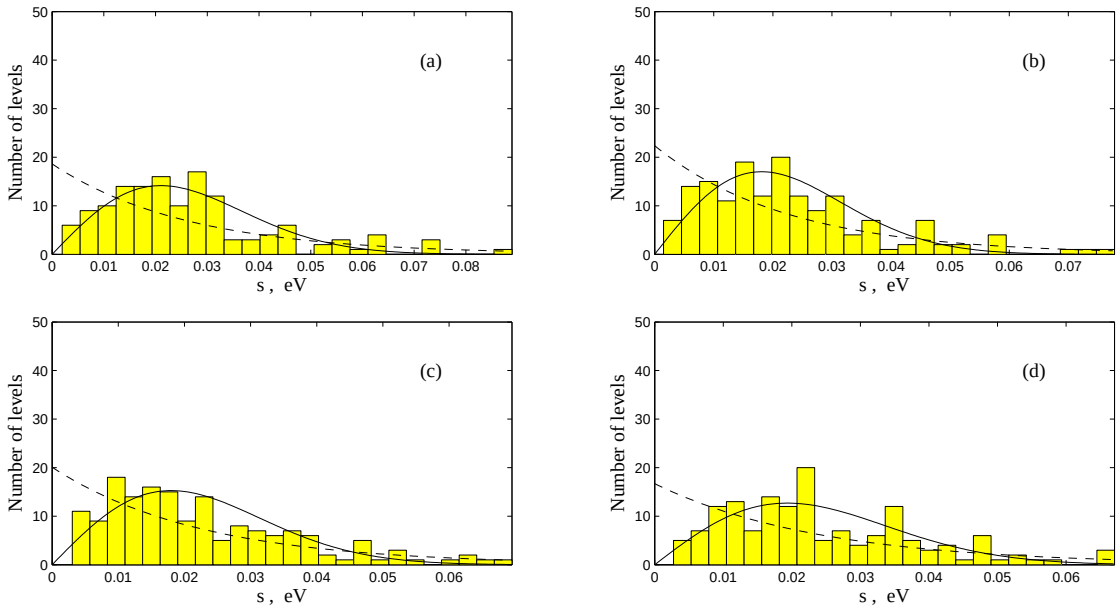

Figure 5. The same as in Figure 3 for the transverse energy domain (21).

3. Conclusion

Wigner distribution (1) of distances between adjacent energy levels of quantum system is the pronounced manifestation of quantum chaos phenomenon. Building of the inter-level distances distribution requires computational methods which allow one to find densely lying eigen-energies in the potential wells with sophisticated configuration. This problem naturally arises under consideration of the axial channeling in the silicon crystal near [110] axis of electrons with energy of some hundreds of MeV and higher. As we demonstrate in the present paper, the spectral method is sufficient and effective for this problem.

The obtained results demonstrate a different degree of agreement between the Wigner distribution and the calculated inter-level distance ones for the different transverse energy ranges. This fact could have some causes like the difference of average inter-level distance for these ranges and presence of regular (in the classic limit) motion domains among the chaotic motion. Anyway, this problem requires further more detailed investigations.

References

[1] Berry M V 1987 *Proc. R. Soc. Lond.* A **413** 183
[2] Stöckmann H-J 2000 *Quantum Chaos. An Introduction* (Cambridge: Cambridge University Press)
[3] Akhiezer A I and Shul'ga N F 1996 *High-Energy Electrodynamics in Matter* (Amsterdam: Gordon and Breach)
[4] Uggerhøj U I 2005 *Rev. Mod. Phys.* **77** 1131
[5] Akhiezer A I, Shul'ga N F, Truten' V I, Grinenko A A and Syshchenko V V 1995 *Physics-Uspekhi* **38** 1119
[6] Feit M D, Fleck J A Jr and Steiger A 1982 *J. Comput. Phys.* **47** 412
[7] Dabagov S, Ognev L I 1988 *Sov. Phys. Tekh. Phys.* **33** 158
[8] Dabagov S, Ognev L I 1988 *Nucl. Instrum. and Methods* B **30** 185
[9] Shul'ga N F, Syshchenko V V and Neryabova V S 2013 *Journal of Surface Investigation. X-ray, Synchrotron and Neutron Techniques* **7** 279
[10] Shul'ga N F, Syshchenko V V and Neryabova V S 2013 *Nucl. Instrum. and Methods* B **309** 153